Thiol-responsive lyotropic liquid crystals exhibit triggered phase re-arrangement and hydrogen sulfide (H_2S) release

Matthew C. Urquhart,[a] Francesca Ercole,[a] Andrew J. Clulow,[a,b] Thomas P. Davis,[a,c] Michael R. Whittaker,[a] Ben J. Boyd*[a,d] and John F. Quinn*[a,e]

a. *Drug Delivery, Disposition and Dynamics Theme, Monash Institute of Pharmaceutical Sciences, Monash University, Parkville, VIC 3052, Australia.*
b. *BioSAXS beamline, Australian Synchrotron, ANSTO, 800 Blackburn Road, Clayton, Victoria 3168, Australia*
c. *Australian Institute for Bioengineering and Nanotechnology, The University of Queensland, Brisbane, Queensland 4072, Australia*
d. *Department of Pharmacy, University of Copenhagen, Universitetsparken 2, 2100 Copenhagen, Denmark*
e. *Department of Chemical Engineering, Faculty of Engineering, Monash University, Parkville, Victoria 3052, Australia.*

Hydrogen sulfide (H_2S) is an important signalling molecule with potential pharmaceutical applications. In pursuit of a suitable delivery system for H_2S, herein we apply an amphiphilic trisulfide to concomitantly alter mesophase behaviour of dispersed lipid particles and enable triggered H_2S release. Amperometric release studies indicate the trisulfide acts as a sustained H_2S donor, with inclusion into the mesophase attenuating release vs neat dispersed trisulfide. Taken together the results highlight the potential for including trisulfide-based additives in stimuli-responsive drug delivery vehicles

1. Introduction

The potential of stimuli-responsive drug delivery systems to enhance therapeutic efficacy and reduce off-target effects for drugs is widely acknowledged.[1] In light of this, there has been significant progress in the development of nanoparticles that, via alterations in their structure or properties, release drugs in response to physical stimuli such as light,[2] magnetic fields,[3, 4] changes in temperature[5] etc., or chemical stimuli such as change in pH.[6] Likewise, biochemical differences between the extra- and intracellular environments can also be exploited to facilitate triggered release once a particle is internalised by a target cell. This approach has inspired a number of responsive drug delivery systems which respond to elevated thiol concentrations in the intracellular compartment.[7] The most common strategy for achieving thiol-responsive behaviour is to incorporate disulfide moieties into the molecular architecture, although recently trisulfide-linked materials have also been suggested as potential thiol-responsive triggers.[8-10]

Trisulfides and disulfides are similar in that they both undergo thiol-exchange reactions, with certain degradation products of thiol-trisulfide exchange being capable of further reaction with thiols to generate hydrogen sulfide (H_2S).[11] Therefore, trisulfide based materials, which can be cleaved by biological thiols such as cysteine and glutathione with concomitant release of H_2S, may function as both an excipient for stimuli responsive drug delivery vehicles and a donor for H_2S, a so-called gasotransmitter with potential therapeutic benefits.[12, 13] In certain instances the co-administration of H_2S with therapeutic drugs has been shown to limit side effects such as doxorubicin (DOX)-induced cardiotoxicity.[14, 15] These results have inspired the development of H_2S-releasing materials, and their application in drug delivery systems.[16, 17] Likewise, there has been increased interest in macromolecular H_2S donors which avoid some of the limitations of traditional small molecule H_2S donors such as poor water solubility.[18-20] As such, research and development of new H_2S releasing materials for drug delivery is of increasing importance.

Lyotropic liquid crystals (LLCs) offer significant advantages in a drug delivery context over traditional dosage forms, including the potential to provide on demand drug delivery and the ability to accommodate drug molecules with a wide range of physicochemical properties.[21] The retention and release of drugs from these materials depends on the dimensions and arrangement of water nano-channels which form within the complex three dimensional structures of self-assembled lipidic amphiphilic molecules in aqueous environments.[22] The formation of specific mesophases including the inverse bicontinuous cubic (V_2), inverse hexagonal (H_2) and inverse micellar (L_2) phases can be regulated by control of the lipid packing.[23] LLC nanomaterials can often be dispersed into submicron-size particles analogous to liposomes, but which possess the internal LLC mesophase structures. Furthermore, the incorporation and activation of stimuli responsive molecules and nanoparticles can enable switching between different LLC phases, which in turn provides the opportunity to trigger and control the release of encapsulated material.[24] Taken together, these attributes make LLCs attractive drug delivery systems.

In this work, we present a thiol-responsive LLC which releases H_2S in the presence of cysteine, whilst simultaneously triggering phase rearrangement. This was achieved by the addition of an amphiphilic trisulfide conjugate with a dodecyl tail and a 1,2-diol head group [3-(dodecyltrisulfanyl)propane-1,2-diol: $C_{12}H_{25}$-SSS-diol, Fig. 1C], which was employed as a phase altering additive in a phytantriol (PHY) lipid system. PHY naturally assembles into inverse bicontinuous cubic (V_2) phases at ambient temperature but the addition of $C_{12}H_{25}$-SSS-diol increases the oil-water interfacial curvature, changing the ambient structures towards inverse hexagonal (H_2) phases. In our previous work we demonstrated the use of a polyethylene glycol–cholesterol conjugate linked by a trisulfide bridge (PEG–

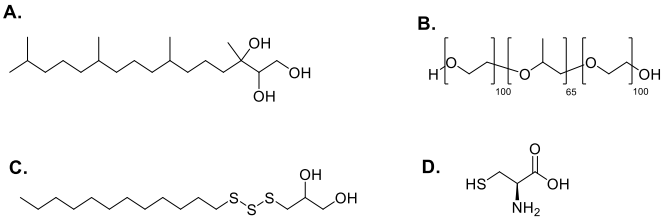

Fig. 1 Molecular structures of (A) phytantriol, (B) Pluronic F127, (C) trisulfide conjugate ($C_{12}H_{25}$-SSS-diol) and (D) cysteine (CYS).

SSS–CHOL) in the preparation of H_2S donating micelles and liposomes.[8] This initial study highlighted the capacity to employ donor moieties as functional linkers that can trigger concomitant reorganisation of nanoscale assemblies. In the current report, we describe the effect of trisulfide incorporation and degradation on lipid mesophase formation, and the associated impact on H_2S release kinetics.

2. Experimental

2.1 Materials

3-(dodecyltrisulfanyl)propane-1,2-diol ($C_{12}H_{25}$-SSS-diol) was synthesised in house, the procedure and characterisation data is provided in the supplementary information. Phytantriol was purchased from DSM Nutritional Products, Singapore. Pluronic ® F127, L-cysteine (97%) and sodium sulfide were purchased from Sigma Aldrich (St Louis, MO, USA). PBS 7.4 (phosphate buffered saline, pH 7.4) was reconstituted from Sigma Aldrich tablets which when dissolved in 1 L of deionized water yields 0.01 M phosphate buffered saline (NaCl 0.138 M, KCl 0.0027 M) pH 7.4 at 25 °C.

2.2 Methods

2.2.1 Sample preparation

Phytantriol and $C_{12}H_{25}$-SSS-diol stock solutions were prepared in chloroform. Appropriate amounts of these stocks were dispensed into 8 mL vials to yield a phytantriol (200 mg) and trisulfide additive (0-8% w/w) mixture. Solvent was evaporated overnight under vacuum. Phytantriol (10% w/w) and trisulfide additive was then dispersed in a pH 7.4 PBS buffer solution (1800 mg, containing 1.5% w/w Pluronic F127) using a Misonix S-4000 tip sonicator (Farmingdale) at 30 amplitude applied for 2 seconds on and 1 second off cycles for 2 minutes total sonication time. To assess the influence of cysteine on the phase behaviour of the samples, 900 µL of the dispersed formulation was mixed with 100 µL of cysteine solution (100 mM) prepared in pH 7.4 PBS. Approximately 48 hours later the formulations were loaded into 1.5 mm quartz capillaries (Charles Supper, Natick, MA) for SAXS measurements at the SAXS/WAXS beamline, Australian Synchrotron ANSTO, Clayton, VIC.

2.2.2 Dynamic light scattering

Dispersed lipid samples were diluted in two fold in PBS and were run at 25 °C on a Malvern Zetasizer ZS series equipped with a 4 mW laser at λ = 633 nm and a detector angle 173° running DTS software. Viscosity and refractive index were assumed to be 0.887 cP and 1.59 as for water and PS latex. Z-average and the polydispersity index (PDI) illustrating the average diameters and size distribution were determined via a cumulants analysis of the measured intensity autocorrelation function by the DTS software.

2.2.3 Small angle X-ray scattering (SAXS)

The internal structure of the lipid phase was assessed using SAXS to evaluate the influence of additive on phase behaviour. All SAXS measurements were performed at the SAXS/WAXS beamline at the Australian Synchrotron. The synchrotron X-ray beam was tuned to a wavelength of 0.953 Å (13.0 keV) at a sample-to-detector distance of 1600 mm which gave the q-range of $0.012 < q < 1.122$ Å^{-1}, where q is the length of the scattering vector defined by $q = (4\pi/\lambda)\sin(\theta/2)$. The sample-to-detector distance was selected to provide good resolution of the diffraction rings from the lipid mesophases, without them being obscured by the intense background scattering observed at low q, close to the beamstop. Whilst the area of the detector is wide enough to measure out to $q = 1.122$ Å^{-1}, diffraction peaks from lipid mesophases are only observed within the range 0.1 Å$^{-1} < q < 0.4$ Å^{-1}, with the rest of the profile being dominated by background scattering. As such, only the q-range containing the diffraction peaks of interest is plotted in the figures of this manuscript.

The 2D scattering patterns were integrated into the 1D scattering function I(q) using the in-house developed software package scatterBrain. Scattering curves are plotted as a function of relative intensity, and phase structures are identified by indexing the Bragg peaks to known relative spacing ratios. The temperature studies utilised a custom capillary holder connected to a water bath.

Kinetic analysis was performed on a sample with 2.5 % w/w additive. 50 µL of freshly prepared cysteine solution in pH 7.4 PBS (100 mM) was added to 450 µL of dispersed formulation. This mixture was then immediately loaded into a quartz capillary for SAXS measurements with frames acquired at one second intervals.

2.2.4 Amperometric H_2S sensing

The H_2S-generating capability of formulations was examined by an amperometric approach using an H_2S selective micro-sensor manufactured by Unisense®. Before measurements were taken the sensor was calibrated by following the manufacture guidelines after a prepolarization period (usually 2 hours or more). Firstly, acidic calibration buffer (pH 4 PBS, 6 ml) was transferred to a sealed 8 ml vial with a custom septum. This was deoxygenated for 20 minutes by bubbling with N_2 gas. The sensor was then immersed into the solution via an opening on the septum. Immediately prior to measurement, a 10 mM stock solution of Na_2S was prepared anaerobically by dissolving a

known quantity of the salt into N_2-flushed, deionized water in a closed container. Calibration points within the expected range of measurement were collected by injecting known amounts of Na_2S stock solution into the stirred calibration buffer solution using a micro-syringe (30-120 µL). The current increased upon addition of the first aliquot and reached a plateau after several seconds. Further calibration values were obtained as subsequent aliquots were added. The recorded data was used to generate a linear calibration plot for [H_2S] vs. current (amps). The calibrated microsensor was used to examine the triggered H_2S-generating capability of pure additive and of additive in dispersed PHY sample as follows.

For the pure additive, a stock solution of $C_{12}H_{25}$-SSS-diol was first prepared by dissolving 3.6 mg in 3.43 mL of DMSO. 200 µL of $C_{12}H_{25}$-SSS-diol was added to 1150 µL of pH 7.4 PBS in a sealed vial and deoxygenated by sparing with nitrogen prior to analysis. To trigger H_2S release, 150 µL of 100 mM cysteine in PBS was added to yield a final trisulfide concentration of 412 µM and final cysteine concentration of 10 mM.

In the case of the lipid formulation, 23 µL (24.3 mg) of the 8 % w/w additive in PHY dispersed sample was diluted in 1327 µL of pH 7.4 PBS in a sealed vial and deoxygenated by sparging with nitrogen prior to analysis. To trigger H_2S release, 150 µL of 100 mM cysteine in PBS was added to yield a final trisulfide concentration of 411 µM and final cysteine concentration 10 mM.

3. Results and discussion

The $C_{12}H_{25}$-SSS-diol additive was synthesised using the sulfur transfer agent, *N,N'*-thiobisphthalimide, to yield the key intermediates as *N*-(alkyl thiosulfenyl)phthalimides (alkyl phthalimido disulfides). Use of such phthalimido intermediates in trisulfide synthesis has been shown to yield products largely free from disulfide and polysulfide products.[10, 25] In the current study, dodecane-1-thiol was reacted with *N,N'*-thiobisphthalimide to yield the intermediate 2-(dodecyldisulfanyl)isoindoline-1,3-dione. The intermediate was subsequently reacted with 1-thioglycerol to yield the target compound with overall yield of 6.7%. Successful synthesis was confirmed by ^1H and ^{13}C NMR spectroscopy and liquid chromatography-mass spectrometry (LC-MS) (Fig. S1-S5).

A range of lipids have been shown to form LLCs in excess water of which PHY has attracted attention due to its chemical stability, rich self-assembly behaviour and sensitivity of structure to additives. PHY forms bicontinuous cubic (V_2) structures at low temperatures, and inverse hexagonal phases (H_2) or disordered inverse micellar (L_2) phases at higher temperatures.[26] To investigate the effect of incorporating various concentrations of $C_{12}H_{25}$-SSS-diol on the equilibrium phase behaviour of dispersed PHY, the additive was first mixed with PHY at concentrations between 0 and 8% w/w, after which

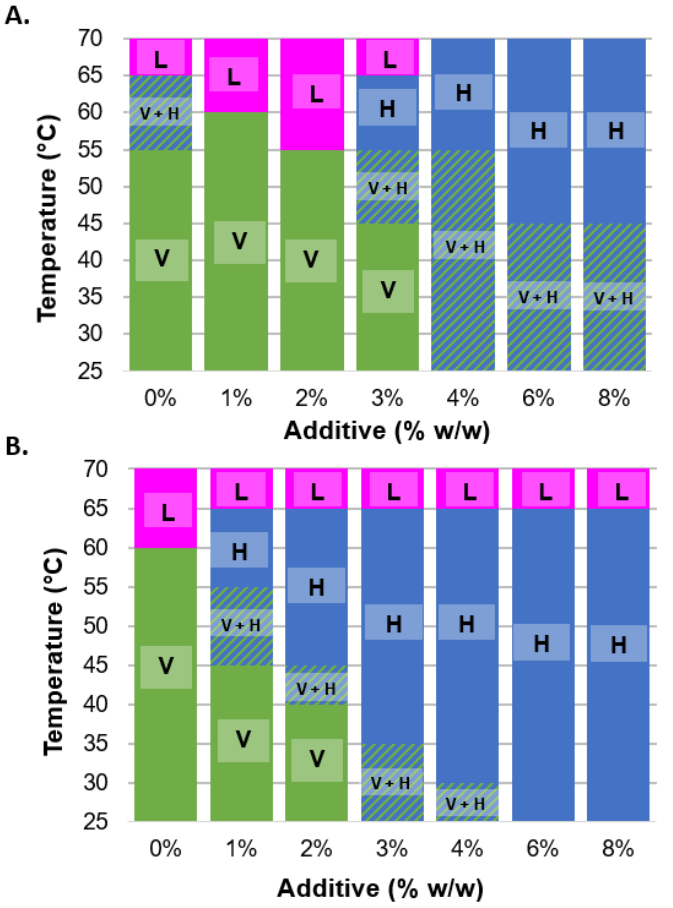

Fig. 2 Representation of mesophase structure of dispersed PHY particles (10% w/w) at temperatures from 25-70°C with various amounts of $C_{12}H_{25}$-SSS-diol additive. A. prior to the addition of cysteine trigger, B. 48 hours after the addition of cysteine (10 mM). Phases identified by comparison of SAXS Braggs peaks with known spacings. V = bicontinuous cubic phase with Pn3m spacegroup, H = inverse hexagonal phase, H_2 and L = disordered inverse micellar phase L_2. Raw scattering profiles found in Fig. S6-S13).

pH 7.4 PBS buffer containing 1.5% w/v Pluronic F127 was added and the lipids were dispersed via tip sonication. The mean particle sizes of the dispersions was found by dynamic light scattering to be inversely related to the amount of additive present. The particles with additive were in the range of 177-232 nm, whilst PHY particles prepared without additive were 247 nm (Table. S1). Self-assembled structures were determined by indexing characteristic Bragg peak spacings measured by small angle X-ray scattering (SAXS) at the Australian Synchrotron. In the absence of $C_{12}H_{25}$-SSS-diol, PHY showed the expected phase behaviour, with formation of the inverse bicontinuous cubic phase with Pn3m spacegroup up to 55°C (indicated by the Bragg peaks at spacing ratios equal to √2, √3, √4, √6 and √8). Above 55 °C, the emergence of an inverse hexagonal phase was observed (Braggs peaks at spacing ratios 1, √3 and √4). At temperatures above 65°C a disordered inverse micellar phase (L_2) formed (Fig. 2 and Fig. S6-S13). Inclusion of small amounts of $C_{12}H_{25}$-SSS-diol induced a concentration-dependent suppression of the temperatures at which the

Pn3m-H_2-L_2 phase transitions occurred. The incorporation of additive resulted in a minor decrease in the lattice parameter of the Pn3m phase at ambient temperature (65.8 -> 63.4 Å) (Fig. S14). A decrease in lattice parameter of each phase with increased temperature was also observed, consistent with previous reports of dispersed PHY particles (Fig. S15).[27] Significantly, the addition of 8% w/w of $C_{12}H_{25}$-SSS-diol to PHY reduces the temperature at which the H_2 phase is first observed from 60 °C to below 25 °C. This effect is analogous to the previously reported addition of vitamin E acetate to PHY, which also causes a concentration dependent depression in the temperature of the cubic Pn3m structure to H_2 phase transition.[28] In both cases, the additive exhibits a reduced volume of the hydrophilic head group relative to its hydrophobic tail portion in comparison to PHY, making the molecule more conical on average. As such, the additives more likely reside in the hydrophobic region of the lipid bilayer, thus imparting a greater negative curvature (curvature towards the aqueous domains in the mesophase) at the oil-water interfaces.

The 'responsiveness' of the structures to a representative thiol trigger (L-cysteine) was studied by addition of the trigger 48 hrs prior to the scattering measurements, summarised in Fig. 2B. As noted in the literature,[11] trisulfides undergo thiol exchange reactions leading to reactive (perthiol, RSSH) intermediates which can undergo reaction with a further equivalent of thiol (cysteine) to yield H_2S and disulfide-cysteine conjugates. This behaviour was confirmed by LCMS for the additive used in this study (Fig. S16-S18). In the cysteine-triggered samples a further reduction in the temperature at which the H_2 phase formed was observed, compared to the non-triggered samples. This effect was again dependent on the concentration of $C_{12}H_{25}$-SSS-diol. The addition of cysteine to the additive-free PHY system induced very minor differences in the phase behaviour. In contrast, addition of cysteine to the sample containing 3% w/w $C_{12}H_{25}$-SSS-diol resulted in a reduction of the temperature at which the H_2 phase was present, from 45°C to below 25 °C. This effect is hypothesised to be caused by a further reduction in the interfacial curvature. The more hydrophobic disulfide degradation product would likely remain in the hydrophobic region of the lipid bilayer, whereas the hydrophilic cysteine adduct would be more likely to disperse into the aqueous surroundings.

The kinetics of the phase transition were further probed to evaluate the appropriateness of the system for physiological application. In this experiment a significant transition from the cubic Pn3m phase to the H_2 phase occurred within two minutes of the addition of cysteine (Fig. 3 and Fig. S19). In this case, the small amount H_2 phase present at the beginning of the experiment, which is not expected according to the equilibrium phase diagram (Fig.2) is likely due minor sample inhomogeneity. Nevertheless, the rapid transition after triggering towards the H_2 phase indicates the system's suitability for physiological

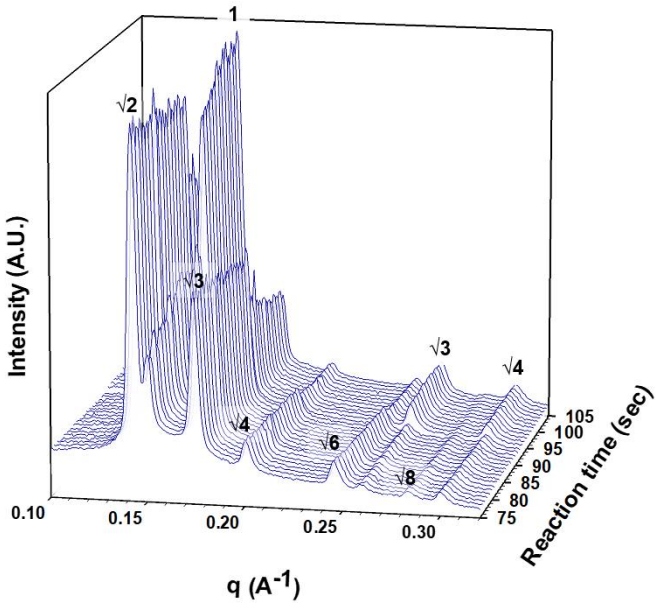

Fig. 3 Small angle X-ray scattering profiles of 2.5% w/w $C_{12}H_{25}$-SSS-diol in PHY formulation after the addition of cysteine trigger at 25°C. Braggs peaks indicating the cubic Pn3m mesophase are labelled with √2, √3, √4, √6 and √8. Peaks indicating the presence of inverse hexagonal phase are labelled as 1, √3 and √4. Time between mixing of the trigger and first data acquisition was 77 seconds.

purposes where the trigger is transiently present or where fast phase transition is required. If the application of the trigger were to concurrently release a drug, this particular additive is not suitable because it drives the system from the 'fast release' cubic phase structure to the 'slow release'-H_2 phase. The change in chemical structure would need to yield more hydrophilic products in response to the trigger to achieve this trajectory in phase behaviour. Nonetheless, the results highlight the responsiveness of trisulfide linkers and the ability to exploit their degradation to trigger changes in phase behaviour.

Further, the kinetics of H_2S release from the trisulfide were determined using amperometric H_2S-selective sensing (Fig. 4). Specifically, the rate of release of H_2S from the additive incorporated into the dispersed PHY particles was compared to the rate of release of H_2S from a similar concentration of free additive in solution. The rate of release of H_2S from the free additive in solution peaked within 30 mins of the addition of the trigger, whereas the release of H_2S from the lipid formulation continued to increase across the full 90 mins of testing. This difference may be attributed to the steric interaction of adjacent PHY groups hindering access of the cysteine to the trisulfide moiety. The controlled and more gradual release of H_2S from the lipid formulation is potentially beneficial given the narrow therapeutic window of H_2S.[29]

4. Conclusion

In summary, a bespoke trisulfide linked conjugate was developed that can serve as a dual functional additive in lipid

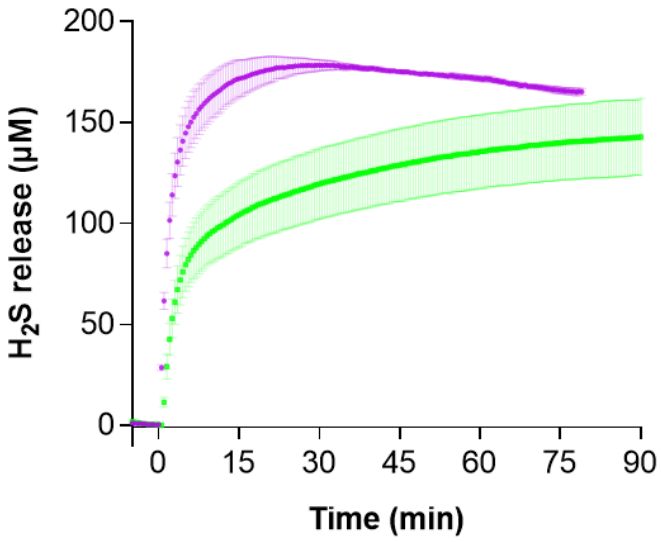

Fig. 4 Release of H_2S measured by an amperometric microsensor after exposure to 10 mM of cysteine solution prepared in pH 7.4 PBS. Purple - $C_{12}H_{25}$-SSS-diol (412 µM). Green - 8% w/w $C_{12}H_{25}$-SSS-diol in PHY (trisulfide – 411 µM). Data are mean ± s.d., n=3.

lyotropic systems, which both modulates the phase behaviour of the system and acts as a donor of H_2S. The synergy between these functions indicates significant potential for further trisulfide use in stimuli responsive LLC systems. Promisingly, studies on the lipid mesophases indicated that relatively small amounts of additive are required to impart stimuli responsive behaviour to PHY dispersions. Furthermore, the often-desired slow and continuous release of H_2S was observed from the formulation. Taken together these results demonstrate the potential of trisulfides as concomitant phase modulators and H_2S donors. The stimuli responsiveness of the additive used in this study represents a key advancement over the reported vitamin E system which inspired this work.[28] This study is the first report of a trisulfide compound as a lipid phase modulator. Further investigation of different trisulfide additives in combination with different lyotropic liquid crystal matrices is required to fine tune the phase formation, opening the door to next-generation drug delivery systems.

This work was carried out within the ARC Centre of Excellence in Convergent Bio-Nano Science and Technology (CE140100036). J. F. Q. is grateful for an ARC Future Fellowship (FT170100144). The small angle X-ray scattering studies described herein were performed on the SAXS/WAXS beamline at the Australian Synchrotron, part of ANSTO. The authors acknowledge support provided to this project from the Australian Synchrotron (Australian Synchrotron Beamtime Application AS2/SAXS/16144). We also wish to acknowledge support provided to this research project by the HMSTrust Analytical Laboratory which is based at the Monash Institute of Pharmaceutical Sciences.

References

1. S. Mura, J. Nicolas and P. Couvreur, *Nat Mater*, 2013, **12**, 991-1003.
2. A. Raza, U. Hayat, T. Rasheed, M. Bilal and H. M. N. Iqbal, *Journal of materials research and technology*, 2019, **8**, 1497-1509.
3. X. Sun, N. Alcaraz, R. Qiao, A. Hawley, A. Tan and B. J. Boyd, *Colloids Surf B Biointerfaces*, 2020, **191**, 110965.
4. X. Sun, J. D. Du, A. Hawley, A. Tan and B. J. Boyd, *Colloids and Surfaces B: Biointerfaces*, 2021, **207**, 112005.
5. M. Karimi, P. Sahandi Zangabad, A. Ghasemi, M. Amiri, M. Bahrami, H. Malekzad, H. Ghahramanzadeh Asl, Z. Mahdieh, M. Bozorgomid, A. Ghasemi, M. R. Rahmani Taji Boyuk and M. R. Hamblin, *ACS Appl. Mater. Interfaces*, 2016, **8**, 21107-21133.
6. R. Negrini, W.-K. Fong, B. J. Boyd and R. Mezzenga, *Chem Commun (Camb)*, 2015, **51**, 6671-6674.
7. J. F. Quinn, M. R. Whittaker and T. P. Davis, *Polymer chemistry*, 2016, **8**, 97-126.
8. F. Ercole, M. R. Whittaker, M. L. Halls, B. J. Boyd, T. P. Davis and J. F. Quinn, *Chem. Commun.*, 2017, **53**, 8030-8033.
9. Y. Yang, B. Sun, S. Zuo, X. Li, S. Zhou, L. Li, C. Luo, H. Liu, M. Cheng, Y. Wang, S. Wang, Z. He and J. Sun, *Science advances*, 2020, **6**.
10. N. V. Dao, F. Ercole, L. M. Kaminskas, T. P. Davis, E. K. Sloan, M. R. Whittaker and J. F. Quinn, *Biomacromolecules*, 2020, **21**, 5292-5305.
11. D. Liang, H. Wu, M. W. Wong and D. Huang, *Organic letters*, 2015, **17**, 4196.
12. R. Wang, *Antioxidants & redox signaling*, 2003, **5**, 493.
13. K. Abe and H. Kimura, *The Journal of neuroscience : the official journal of the Society for Neuroscience*, 1996, **16**, 1066.
14. X.-Y. Wang, C.-T. Yang, D.-D. Zheng, L.-Q. Mo, A.-P. Lan, Z.-L. Yang, F. Hu, P.-X. Chen, X.-X. Liao and J.-Q. Feng, *An International Journal for Chemical Biology in Health and Disease*, 2012, **363**, 419-426.
15. Y. Wang, K. Kaur, S. J. Scannelli, R. Bitton and J. B. Matson, *Journal of the American Chemical Society*, 2018, **140**, 14945.
16. Z. J. Song, M. Y. Ng, Z.-W. Lee, W. Dai, T. Hagen, P. K. Moore, D. Huang, L.-W. Deng and C.-H. Tan, *Med. Chem. Commun.*, 2014, **5**, 557-570.
17. Y. Zheng, B. Yu, L. K. La Cruz, M. Roy Choudhury, A. Anifowose and B. Wang, *Journal*, 2018, **38**, 57-100.
18. M. C. Urquhart, F. Ercole, M. R. Whittaker, B. J. Boyd, T. P. Davis and J. F. Quinn, *Polym. Chem.*, 2018, **9**, 4431-4439.
19. L. Connal, *Journal of Materials Chemistry. B, Materials for Biology and Medicine*, 2018, **6**, 7122-7128.
20. K. Kaur, R. J. Carrazzone and J. B. Matson, *Antioxidants & Redox Signaling*, 2020, **32**, 79-95.
21. C. J. Drummond and C. Fong, *Current Opinion in Colloid & Interface Science*, 1999, **4**, 449-456.
22. K. W. Y. Lee, T.-H. Nguyen, T. Hanley and B. J. Boyd, *International Journal of Pharmaceutics*, 2009, **365**, 190-199.
23. J. N. Israelachvili, D. J. Mitchell and B. W. Ninham, *Journal of the Chemical Society, Faraday Transactions 2: Molecular and Chemical Physics*, 1976, **72**, 1525-1568.
24. W.-K. Fong, R. Negrini, J. J. Vallooran, R. Mezzenga and B. J. Boyd, *Journal of Colloid And Interface Science*, 2016, **484**, 320-339.
25. N. V. Dao, F. Ercole, M. C. Urquhart, L. M. Kaminskas, C. J. Nowell, T. P. Davis, E. K. Sloan, M. R. Whittaker and J. F. Quinn, *Biomater Sci*, 2021, **9**, 835-846.
26. J. Barauskas and T. Landh, *Langmuir*, 2003, **19**, 9562-9565.
27. N. R. Yepuri, A. J. Clulow, R. N. Prentice, E. P. Gilbert, A. Hawley, S. B. Rizwan, B. J. Boyd and T. A. Darwish, *J Colloid Interface Sci*, 2019, **534**, 399-407.

28. Y.-D. Dong, I. Larson, T. Hanley and B. J. Boyd, *Langmuir*, 2006, **22**, 9512-9518.
29. A. Stein and S. M. Bailey, *Redox Biol*, 2013, **1**, 32-39.